JOURNAL OF
Materials
CHEMISTRY

One-dimensional double chain composed of carbamoylmethylthio-substituted TTF-based donor in ion radical salt

Go Ono,[a] Hiroshi Terao,[a] Saburo Higuchi,[a] Tadashi Sugawara,*[a] Akira Izuoka[b] and Tomoyuki Mochida[c]

[a]Department of Basic Science, Graduate School of Arts and Sciences, the University of Tokyo, Komaba, Meguro, Tokyo, 153-8902, Japan. E-mail: suga@pentacle.c.u-tokyo.ac.jp
[b]Department of Materials and Biological Sciences, Faculty of Science, Ibaraki University, Bunkyo, Mito, Ibaraki, 310-8512, Japan
[c]Department of Chemistry, Faculty of Sciences, Toho University, Miyama, Funabashi, Chiba, 274-8510, Japan

Received 7th June 2000, Accepted 31st July 2000
First published as an Advanced Article on the web 13th September 2000

Carbamoylmethylthio-substituted TTF-based donors afforded inclusion-type salts with a BF_4 counter ion or an F_4-TCNQ acceptor. The crystal structures of these salts are characterized by a one-dimensional double chain composed of singly-oxidized donors *via* SOMO–SOMO interaction and *side-by-side* S···S contacts. Counter ions of BF_4 are hydrogen-bonded to the amide groups. On the other hand, F_4-TCNQ acceptors are stacked in a channel created by a stair-like arrangement of donor chains. The thermally activating magnetic susceptibility of the F_4-TCNQ complex was interpreted in terms of a double-chain frustrated spin system.

Introduction

Organization of the molecular arrangement in charge transfer complexes is crucial for controlling their physical properties because they strongly depend on the relative orientation of donors and/or acceptors. When neutral donors, such as pyrene,[1] perylene,[2] or BEDT-TTF (BEDT = bis(ethylenedithio)-TTF),[3] *etc.*, self-assemble, they form a dimeric herringbone structure due to the quadrupolar interaction. On the other hand, when donors are singly oxidized, they tend to form a dimer or a stacking structure due to the attractive SOMO–SOMO interaction.[4]

In order to create a characteristic molecular arrangement of donors, we have been interested in introducing an additional intermolecular interaction to the aforementioned π–π interaction. Intermolecular hydrogen bonds are possible candidates. Some examples of crystal structures and properties of donors with a hydrogen-bonding group have been reported.[5] Bryce *et al.* synthesized 1 : 1 radical-ion salts of a TTF derivative carrying a thioamide group.[6] In this salt, an intermolecular hydrogen bond was formed between a thioamide group and a bromide anion. Batail *et al.* prepared a donor substituted with a chiral alcohol group.[7] This donor (D) constructed a DDAA stack with TCNQ (A) in the 1 : 1 complex as a result of the formation of intermolecular hydrogen bonds.

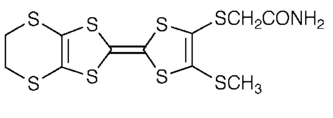

AMET

On the basis of these results, we prepared a BEDT-TTF derivative, AMET, carrying a carbamoylmethylthio group ($–SCH_2CONH_2$), and found that a polymeric hydrogen bond is formed along the perpendicular direction to the donor plane due to the conformational flexibility of the carbamoylmethyl group.[8] On the other hand, in charge transfer complexes or radical ion salts of AMET, the intermolecular interaction between donors becomes attractive as described above. Therefore, it is interesting to see whether this attractive interaction and the hydrogen bond of the carbamoylmethyl group operate cooperatively to form a unique crystal structure or not.

In this paper, supramolecular crystal structures of an ion radical salt and a charge transfer complex of AMET will be described, paying attention to the variation of intermolecular interactions from the aspect of crystal engineering. In the salts, counter ions or acceptors are incorporated in a cavity or in a channel created by a hydrogen-bonding scheme composed of AMETs. It was found that a one-dimensional double-chain arrangement of the singly oxidized AMETs was observed in both the radical ion salt and the charge transfer complex of AMET. The interesting magnetic properties of the CT complex are also discussed on the basis of the double-chain frustrated spin system.

Results

Crystal structure of 1 : 1 salt of AMET·BF_4

A crystal structure of the 1 : 1 salt of AMET·BF_4, which is prepared through electro-crystallization of AMET in the presence of $Bu^n{}_4N \cdot BF_4$, is shown in Fig. 1. Conformation of the carbamoylmethyl group is (−sc)-(−sc)-(+sp) viewed from the donor moiety, and two counter ions (BF_4^-) are sandwiched by the two donor planes. The BF_4^- ions are hydrogen-bonded to the amide units with N–H···F distances of 3.24 Å and 3.28 Å (Fig. 2a). The long axes of the pairing donors which incorporate counter ions are perpendicular to each other (Fig. 2b). These anion-incorporating units are arranged in an array along the (1 0 −1) direction, and these arrays are located on the *ac* plane (Fig. 1).

Furthermore, each of the donor planes forms a *face-to-face* dimer with that of the neighboring pair, respectively (Fig. 3). The distances of the close S···S contacts between two facing TTF moieties are 3.47, 3.50 and 3.67 Å. It is noted that these dimers align *side-by-side* along the *b* axis with the S···S contacts of 3.59 Å and 3.68 Å between a sulfur atom of the carbamoylmethylthio group and sulfur atoms of the donor

DOI: 10.1039/b004557h

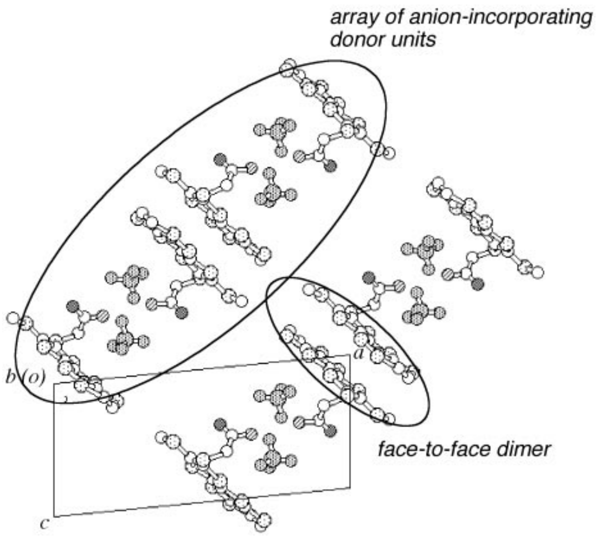

Fig. 1 Crystal structure of the 1 : 1 salt of AMET·BF_4 viewed along the *b* axis.

moiety. Thus, one-dimensional double-chains of donors are constructed along the *b* axis (Fig. 3).

Crystal structure of the AMET·F_4-TCNQ complex

Crystals of the charge transfer complex of AMET and F_4-TCNQ (1 : 1 ratio of donor to acceptor) were prepared by slow-evaporation from a solution of 1,1,2-trichloroethane. A crystal structure of AMET·F_4-TCNQ salt is shown in Fig. 4. In the salt, the carbamoylmethyl group of AMET is folded towards the perpendicular direction in reference to the donor plane with the (+sc)-(+sc)-(+sc) conformation viewed from the donor moiety (Fig. 5a). In contrast to AMET·BF_4 salts, the carbamoylmethyl groups of facing AMETs are hydrogen-bonded directly. The intermolecular hydrogen-bond distance between amide groups (N–H···O=C) is 2.96 Å (Fig. 5b), a relatively weak hydrogen bond. The average distance of hydrogen bonds with an amide group is 2.81 Å. The hydrogen bonds between the carbamoylmethyl groups connect donors to constitute a molecular staircase (Fig. 4).

Each donor in the hydrogen-bonded dimer interacts with an adjacent donor in a *face-to-face* manner as in the case of the 1 : 1 salt of AMET·BF_4, the distances of S···S contacts between the facing dimer are 3.42 and 3.46 Å. The dimers also align along the *a* axis with *side-by-side* S···S contacts of 3.57, 3.73, and 3.76 Å (Fig. 6). Thus one-dimensional double chain structure of $AMET^{+\cdot}$ is also recognized in this salt.

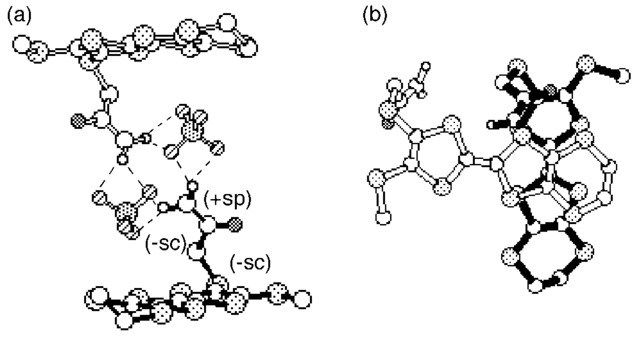

Fig. 2 Structure of a dimer containing BF_4 anions through hydrogen bonds with carbamoylmethyl group. (a) Hydrogen bonds between two amide units and two BF_4 anions. The distances between N–H···O are 3.24, 3.28 Å. (b) Relative orientation of donor planes of AMETs within a dimer. BF_4 anions are omitted for clarity.

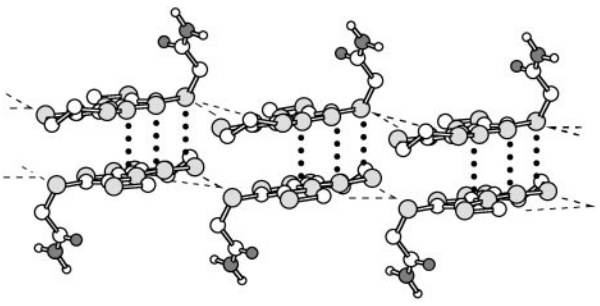

Fig. 3 One-dimensional double-chain structure of AMET in the 1 : 1 salt of AMET·BF_4. There are S···S contacts in the *face-to-face* dimer of donors (dotted lines; 3.47, 3.50 and 3.67 Å) and *side-by-side* along the *b* axis (broken lines; 3.59, 3.68 Å).

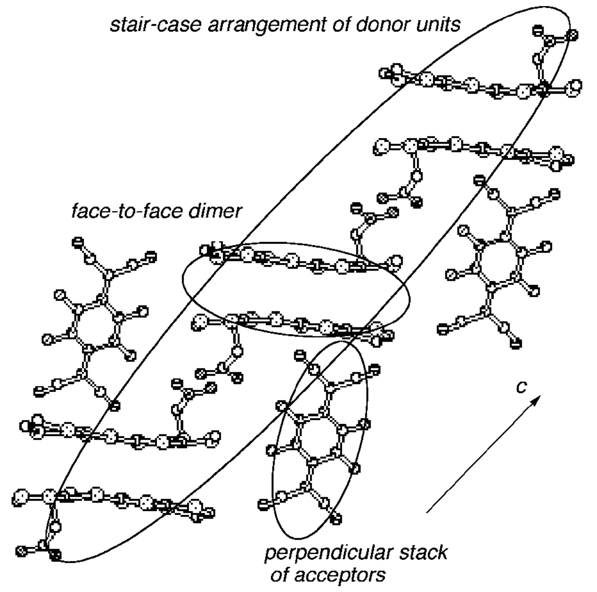

Fig. 4 Crystal structure of AMET·F_4-TCNQ salt viewed along the *c* axis.

On the other hand, F_4-TCNQ is stacked along the *a* axis. The stacking direction of acceptors is perpendicular to the donor plane, and is parallel to the direction of the one-dimensional chain. In this stacking, acceptors are strongly dimerized, the intra- and interdimer distances being 3.15 and 3.40 Å, respectively.

Conductive behavior of AMET salts

Reflecting the 1 : 1 ratio of the donor and the counter ion, the salt of AMET·BF_4 is almost an insulator, and the conductivity of the salt at room temperature is as low as 10^{-7} S cm^{-1}. The AMET·F_4-TCNQ salt also exhibits a poor conductivity ($\sigma_{rt} = 1.4 \times 10^{-5}$ S cm^{-1}).

Another ion-radical salt of AMET and BF_4 anion was obtained by electro-crystallization in the presence of an aliquot of water. The donor to acceptor ratio was determined to be 2 : 1 based on the elemental analysis, although the crystal structure of the 2 : 1 salt was not revealed due to the poor crystallinity. The conductivity of the 2 : 1 salt ($\sigma_{rt} = 5$ S cm^{-1}) is about 10^6 times higher than that of the 1 : 1 salt.

Magnetic properties of AMET salts

The magnetic properties of the 1 : 1 salt of AMET·BF_4 and the AMET·F_4-TCNQ salt were measured with an EPR spectrometer and a SQUID magnetometer. The magnetic behaviors of these salts turned out to be totally different, although the arrangements of AMET molecules are similar to each other.

Temperature dependence of the magnetic susceptibility of the polycrystalline sample of AMET·BF_4 salt showed the only Curie-type susceptibility at temperatures lower than 30 K. Since

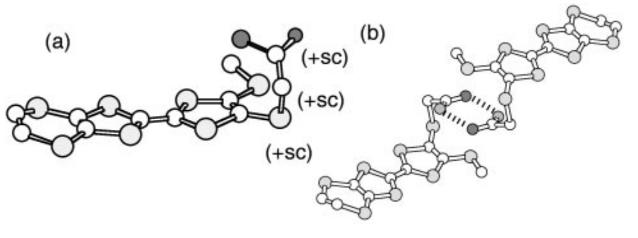

Fig. 5 (a) Conformation of carbamoylmethyl group of AMET in AMET·F_4-TCNQ salt. (b) Hydrogen-bonded *head-to-head* dimer of AMET (N–H···O distance; 2.96 Å).

the magnitude of the detected spin density is less than 1% of the total spin of the cation-radical of AMET, the magnetic susceptibility may be due to the paramagnetic impurity.

On the other hand, the EPR spectrum of AMET·F_4-TCNQ in the temperature range 50–275 K showed a thermally populated signal with the anisotropic g values ($g_1 = 2.0112$, $g_2 = 2.0062$, $g_3 = 2.0024$). From the g-values, the signal was assigned to the cation-radical of AMET (Fig. 7a). This anisotropic signal became averaged ($g_{av} = 2.0064$) at temperatures higher than 160 K, presumably due to dynamic processes. An additional sharp signal at $g = 2.0029$ appeared with thermal excitation at temperatures higher than 300 K (Fig. 7b). The new signal was assigned to the anion radical of F_4-TCNQ because the g-value of the latter was reported to be 2.0028.

The magnetic susceptibility (χ) of AMET·F_4-TCNQ was measured with a SQUID magnetometer (Fig. 8). In addition to the magnetic susceptibility from the paramagnetic impurity at temperatures lower than 30 K, the thermally activating susceptibility was detected in the temperature range of 50–280 K, the χ value remained constant in this temperature range. From the Curie constant, the magnitude of the detected spin density was evaluated to be about 30% of the total spin of $\text{AMET}^{+\bullet}$. At temperatures higher than 280 K, the χ value started to increase exponentially. On the basis of the EPR assignment in the respective temperature range, the magnetic susceptibility at 60–280 K is assigned to the cation-radical of AMET, whereas the magnetic susceptibility at temperatures higher than 280 K is assigned to both the anion radical of F_4-TCNQ and the cation-radical.

Discussion

Characteristics of crystal structures of AMET·BF_4 and AMET·F_4-TCNQ

In the crystal of the 1 : 1 salt of AMET·BF_4, the multi-centered hydrogen bonds are formed between carbamoylmethyl groups of facing AMETs and two BF_4 anions (Fig. 1). The hydrogen-bonding scheme may be caused by the higher proton-accepting ability of the BF_4 anion compared with that of the carbamoylmethyl group. On the other hand, a singly oxidized donor tends to form a *face-to-face* dimer on the basis of the attractive SOMO–SOMO interaction of the donor units. Furthermore, the *face-to-face* dimers arrange *side-by-side* due to the attractive S···S interactions to form a double-chain structure (Fig. 3).

In contrast, hydrogen bonds are formed directly between carbamoylmethyl groups of the neighboring donors in the AMET·F_4-TCNQ crystal (Fig. 4). Although primary amides, in general, form doubly hydrogen-bonded chains,[9] only one proton of the amide unit of AMET is used for the intermolecular hydrogen bond between amide units. The other forms a weak hydrogen bond with the fluorine atom of F_4-TCNQ. The columns of F_4-TCNQ are located in channels created by the staircase arrangement of donors. The donors form a *face-to-face* dimer, and the dimer arranges *side-by-side* to form a double-chain structure Fig. 6 as in the case of the BF_4 salt.

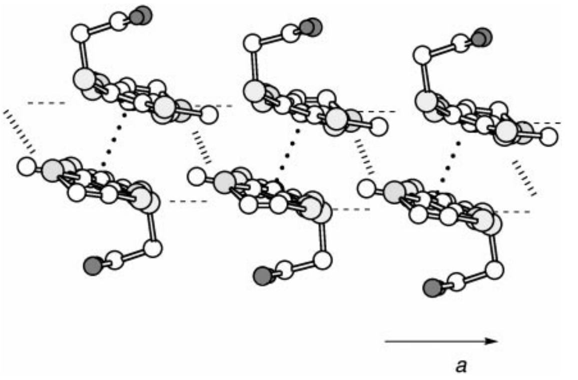

Fig. 6 One-dimensional double-chain structure constituted by vertical and horizontal S···S contacts in AMET·F_4-TCNQ salts. The *face-to-face* S···S contacts of donors (dotted lines) are 3.42, 3.46 Å. The *side-by-side* S···S contacts between donors (broken line) are 3.57, 3.73 and 3.76 Å.

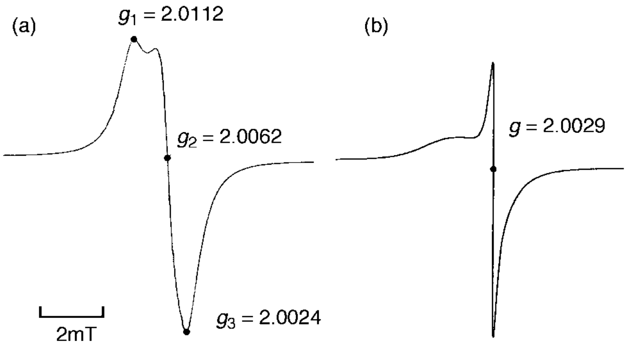

Fig. 7 EPR spectrum of the AMET·BF_4-TCNQ complex at (a) 90 K, (b) 310 K.

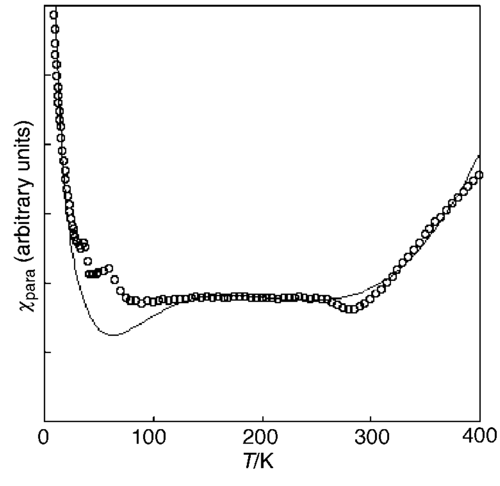

Fig. 8 Temperature dependence of the paramagnetic susceptibility of AMET·F_4-TCNQ. The solid line is a theoretical fit of the sum of the terms of thermally populated triplets derived from the donor ($C = 0.115$ emu K mol^{-1}, $J = -150$ K) and that from the acceptor ($C = 0.375$ emu K mol^{-1}, $J = -1270$ K), and the Curie impurity.

When the arrangement of the double-chain structures in BF_4 and F_4-TCNQ salts are examined closely, there are some differences in the intrachain interactions. As far as the *face-to-face* interaction of the donor units is concerned, the degrees of the interactions of both salts are almost the same. On the other hand, the *side-by-side* interaction in AMET·BF_4 is significantly smaller than that in AMET·F_4-TCNQ. Namely, in the BF_4

salt, the interaction is observed only between the sulfur atom of the carbamoylmethyl group and those of the ethylenedithio moiety of the neighboring donor, while in the F_4-TCNQ complex the interactions in three sites are observed between ethylenedithio moieties (Fig. 6). Consequently, the dimeric interaction in the AMET·BF_4 salt predominates over the *side-by-side* interaction. In contrast, two kinds of interactions are comparable in AMET·F_4-TCNQ, and the arrangement of the latter can be regarded as a *two-leg-ladder type*. It is to be stressed that such a characteristic double-chain structure composed of donors is well isolated from each other by virtue of the carbamoylmethyl groups.

Magnetic interaction in AMET·BF_4 and AMET·F_4-TCNQ

Although the donor arrangements in both AMET·BF_4 and AMET·F_4-TCNQ can be characterized by the one-dimensional double-chain structure, there is a distinct difference in the anisotropic intrachain interaction. Thus it is intriguing to compare the magnetic properties of these salts.

In the AMET·BF_4 salt, AMET exists as a cation radical since the ratio of the donor to the counter ion is 1 to 1. The degree of the charge transfer in AMET·F_4-TCNQ can also be examined on the basis of the oxidation potential of AMET (0.51 V) and the reduction potential of F_4-TCNQ (0.53 V).[10] Since the difference between the redox potentials is almost nil, the complex is considered to exist as an ion-radical salt according to Torrance's criterion.[11] As a result, it may be concluded that AMET also exists as the cation radical in the F_4-TCNQ salt.

In the case of the polycrystalline sample of AMET·BF_4 salt, only Curie-type susceptibility due to the impurity paramagnetism is detected by EPR at temperatures lower than 50 K. The result suggests that the antiferromagnetic interaction in the *face-to-face* dimer is considerably larger and the thermally excited spins can not be observed even at temperatures higher than 300 K.

On the other hand, two types of thermally activated spins contribute to the paramagnetic susceptibility of AMET·F_4-TCNQ: one originates from the double-chain arrangement of AMET$^{+\cdot}$s and the other is from the stack of F_4-TCNQ. The temperature dependence of the paramagnetic susceptibility in the temperature range in 50–280 K should be interpreted in terms of the spin system which is intrinsic to the double-chain arrangement of donors. In order to discuss the spin system in AMET·F_4-TCNQ more precisely, the overlap integrals along the S···S contacts are calculated by an extended Hückel method. The overlap integral along the rung ($S_a = 40 \times 10^{-3}$) is one-order larger than that along the leg of the ladder ($S_b = 3.0 \times 10^{-3}$). It is to be noted that there is a significant interaction along the diagonal direction ($S_c = 3.3 \times 10^{-3}$) and its magnitude is almost the same as S_b (Fig. 9). Therefore the spin system of AMET·F_4-TCNQ is not a typical *two-leg-ladder*,[12] but it should be designated as a frustrated double-chain composed of the triangle lattices (Fig. 9). Judging from the estimated overlap integrals, the degree of the antiferromagnetic interaction along the rung (J_1) must be much larger than the other two (J_2, J_3), J_2, J_3 can be approximated to be the same ($J_2 = J_3$). The paramagnetic susceptibility, therefore, may be approximated by a Singlet–Triplet (ST) model. The experimental plot of the temperature dependence of the susceptibility was reasonably well reproduced by $J = -50$ K with a negative Weiss temperature of $\theta = -9$ K as shown in Fig. 8. The theoretical model of the frustrated double chain is analyzed by a classical Ising model (See Appendix).

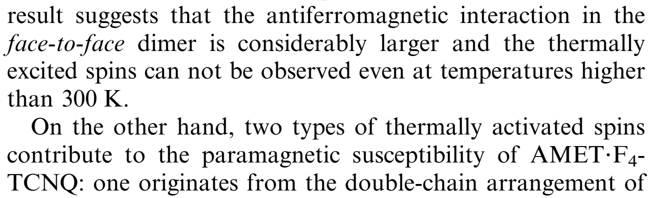

Fig. 9 Frustrated double-chain spin system. Spins in the upper leg are denoted as σ_i and those in the lower are τ_i. Magnetic coupling between σ_i and τ_i is denoted J_1 and those between σ_i and σ_{i+1}, τ_i and τ_{i+1}, and σ_i and τ_{i+1} are J_2.

On the other hand, the thermally activating spins observed at temperatures higher than 300 K may arise from the stacks of anion radicals of F_4-TCNQ, and the plot in this temperature range can be simulated by a ST model with $J = -1270$ K.

Experimental

Materials

Dichloromethane and 1,1,2-trichloroethane were treated with sulfuric acid, then washed with saturated $NaHCO_3$ solution, water and brine, successively. Solvents were distilled prior to use after drying over $CaCl_2$ for several hours at room temperature. AMET was prepared according to a known procedure.[8]

The 1 : 1 radical ion salts of AMET·BF_4 were prepared through electro-crystallization using $Bu^n{}_4N \cdot BF_4$ as a supporting electrolyte. In the anodic side of a 20 mL H-type cell, 8.6 mg (20 μmol) of AMET was dissolved in a mixture of 1,1,2-trichloroethane (5 mL) and dichloromethane (5 mL). In the cathodic side, 65.9 mg (0.20 mmol) of $Bu^n{}_4N \cdot BF_4$ was dissolved in the same mixture of solvents (10 mL). Galvanostatic electro-crystallization was carried out under an electric current of 0.5–1.0 μA for fifteen days to give black single crystals with a block shape. Elemental Analysis, Calc. for $C_{11}H_{11}ONS_8BF_4$ C, 25.58; H, 2.15; N, 2.71; S, 49.66 (%), Found C, 25.65; H, 2.65; N, 2.83; S, 48.58 (%).

The 2 : 1 radical ion salts were also obtained by electro-crystallization using $Bu^n{}_4N \cdot BF_4$ as a supporting electrolyte. In the anodic side of a 20 mL H-type cell, 8.6 mg (20 μmol) of AMET was dissolved in a mixture of 1,1,2-trichloroethane (5 mL) and 1,1,1-trichloroethane (5 mL). In the cathodic side, 65.9 mg (0.20 mmol) of $Bu^n{}_4N \cdot BF_4$ was dissolved in the same mixture of solvents (10 mL). In both sides of the cell, an aliquot of boiled water was added and the cell was left to stand overnight. Galvanostatic electro-crystallization was carried out under an electric current of 0.5–1.0 μA for fifteen days to give dark brown single crystals with a needle shape. Elemental analysis, Calc. for $C_{22}H_{22}O_2N_2S_{16}BF_4$ C, 27.30; H, 2.34; N, 2.96; S, 54.21 (%), Found C, 28.01; H, 2.78; N, 3.10; S, 54.21 (%).

Crystals of the charge transfer complex of AMET and F_4-TCNQ were prepared by slow-evaporation from a solution of 1,1,2-trichloroethane. In 20 mL flasks, 4.3 mg (10 μmol) of AMET and 2.8 mg (10 μmol) of F_4-TCNQ were dissolved in 10 mL of 1,1,2-trichloroethane, respectively. Both solutions were mixed in a 30 mL flask and the mixture was left for ten minutes. Then the solution was filtrated and kept in a refrigerator for ten days to give black needles. Elemental Analysis, Calc. for $C_{23}H_{11}ON_5S_8F_4$ C, 39.14; H, 1.57; N, 9.92; S, 35.61; F, 10.77 (%), Found C, 38.72; H, 1.88; N, 9.96; S, 35.61; F, 10.71 (%).

Electric conductivity measurements

The electric conductivities of single crystals of the AMET·F_4-TCNQ complex, AMET·BF_4, and AMET$_2$·BF_4 were measured by four- or two-probe methods in air. Gold wires (25 μm ϕ) were attached to the sample with gold paste as a contact: along the *a* axis for the AMET·F_4-TCNQ complex, and along the *b* axis for the AMET·BF_4 salt and along the longest axis of the single crystal as grown for the AMET$_2$·BF_4 salt. The sample was fixed in a chamber in a homemade cryostat and was cooled slowly. Temperatures were measured by a (0.03-atom% Fe)–gold-Chromel thermocouple.

EPR spectroscopy

A JEOL JES-TE300 spectrometer was used to record X-band EPR spectra. Temperatures were controlled by a Scientific Instruments digital temperature controller model 9650.

Magnetic measurement

Magnetic susceptibilities of AMET·F_4-TCNQ were measured by a Quantum Design MPMS-XL SQUID system at the field strength of 0.5 T in the temperature range 1.8–400 K. The powder samples of AMET·F_4-TCNQ (22.0 mg) were wrapped in plastic capsule and held in a plastic straw.

X-Ray crystallographic analysis†

AMET·BF_4 radical ion salt: $C_{11}H_{11}NOS_8F_4B$, $M=516.50$, monoclinic, $a=20.944(5)$, $b=9.861(2)$, $c=9.404(2)$ Å, $\beta=95.61(2)°$, $V=1932.9(8)$ Å^3, $T=296(1)$ K, space group $P2_1/a$ (no. 14), $Z=4$, μ(Mo-Kα)$=4.07$ mm^{-1}, 5106 reflections measured, 4955 unique (Rint$=0.0030$). The structure was solved by direct methods using SIR92[13] and expanded using Fourier techniques. The refinement was performed by a full-matrix least-squares method based on 2945 observed reflections ($I>3.00\sigma(I)$). Final refinement with anisotropic thermal factors for all atoms; 235 parameters, $R=0.056$ and $R_w=0.088$.

AMET·F_4-TCNQ salt: $C_{23}H_{11}F_4N_5OS_8$, $M=705.85$, triclinic, $a=7.5773(8)$, $b=13.554(1)$, $c=14.216(1)$ Å, $\alpha=76.894(8)°$, $\beta=85.153(8)°$, $\gamma=74.656(9)°$, $V=1370.9(2)$ Å^3, $T=296(1)$ K , space group $P\bar{1}$ (no. 2), $Z=2$, μ(Cu-Kα)$=0.71$ mm^{-1}, 5786 reflections measured, 5597 unique ($R_{\text{int}}=0.067$). The structure was solved by direct methods using SIR92[14] and expanded using Fourier techniques. The refinement was performed by a full-matrix least-squares method based on 2079 observed reflections ($I>3.00\sigma(I)$). Final refinement with anisotropic thermal factors for all atoms; 370 parameters, $R=0.072$ and $R_w=0.077$.

The atomic scattering factors used throughout were those listed in International Tables for X-ray Crystallography (1974). All calculations were performed using the teXsan crystallographic software package of Molecular Structure Corporation.

Conclusion

In conclusion, the newly developed TTF derivative, AMET, carrying a carbamoylmethyl group was found to afford an inclusion-type crystals, and counter ions or acceptors are included in the cavity or in the channel created by hydrogen-bonded AMETs. Introduction of the carbamoylmethyl group turned out to be effective in the construction of one-dimensional double-chain donors as seen in AMET·BF_4 and AMET·F_4-TCNQ salts. It is to be stressed that the arrangement of donors in radical-ion salts and charge transfer complexes are totally different from that of the neutral complex. This tendency suggests that the predominating adherence force alters from hydrogen bonds to SOMO–SOMO interactions when the AMET is singly oxidized. Reflecting the arrangement of donors in AMET·F_4-TCNQ salt, the temperature dependence of the paramagnetic susceptibility of the salt was found to be interpreted reasonably well in terms of the frustrated double-chain spin system.

Appendix

The frustrated double chain spin system can be theoretically analyzed using an Ising Hamiltonian, with parameters J_1 and J_2 as shown in Fig. 9.

Under the external magnetic field $\boldsymbol{H}$, the partition function Z at temperature T is given by

$$Z(\boldsymbol{H},T)=\sum_{\sigma_i,\tau_i=\pm\frac{1}{2}} e^{-\frac{1}{k_BT}\mathscr{H}(\sigma_i,\tau_i,H)} \tag{1}$$

$$\mathscr{H}(\sigma_i,\tau_i,\boldsymbol{H})=-J_1\sum_i\sigma_i,\tau_i-J_2\sum_i(\sigma_i\sigma_{i+1}+\tau_i\tau_{i+1})$$
$$-J_2\sum_i\sigma_i,\tau_{i+1}-g\boldsymbol{H}\mu_B\sum_i(\sigma_i+\tau_i) \tag{2}$$

The transfer matrix, $\boldsymbol{T}$, where $j_{1,2}=J_{1,2}/k_BT$, $h=g\mu_B\boldsymbol{H}/k_BT$, is defined as below.

$$T=\begin{pmatrix} e^{\frac{1}{4}j_1+\frac{3}{4}j_2-h} & e^{\frac{1}{4}j_1+\frac{1}{4}j_2-h} & e^{\frac{1}{4}j_1-\frac{1}{4}j_2-h} & e^{\frac{1}{4}j_1-\frac{3}{4}j_2-h} \\ e^{-\frac{1}{4}j_1-\frac{1}{4}j_2} & e^{-\frac{1}{4}j_1+\frac{1}{4}j_2} & e^{-\frac{1}{4}j_1-\frac{1}{4}j_2} & e^{-\frac{1}{4}j_1+\frac{1}{4}j_2} \\ e^{-\frac{1}{4}j_1+\frac{1}{4}j_2} & e^{-\frac{1}{4}j_1-\frac{1}{4}j_2} & e^{-\frac{1}{4}j_1+\frac{1}{4}j_2} & e^{-\frac{1}{4}j_1-\frac{1}{4}j_2} \\ e^{\frac{1}{4}j_1+\frac{3}{4}j_2+h} & e^{\frac{1}{4}j_1-\frac{1}{4}j_2+h} & e^{\frac{1}{4}j_1+\frac{1}{4}j_2+h} & e^{\frac{1}{4}j_1+\frac{3}{4}j_2+h} \end{pmatrix} \tag{3}$$

The columns in the matrix are labeled by $(\sigma_i,\ \tau_i)=(+1/2,\ +1/2)$, $(+1/2,\ -1/2)$, $(-1/2,\ +1/2)$, and $(-1/2,\ -1/2)$, while rows are labeled by $(\sigma_{I+1},\ \tau_{I+1})$.

Under the periodic boundary condition, the partition function Z for N spin pairs can be written as a product of 4×4 transfer matrices.

$$Z=\sum_{\sigma_i,\tau_i=\pm\frac{1}{2}}\langle\sigma_N\tau_N|T|\sigma_{N-1}\tau_{N-1}\rangle\cdots$$
$$\langle\sigma_2\tau_2|T|\sigma_1\tau_1\rangle\langle\sigma_1\tau_1|T|\sigma_N\tau_N\rangle \tag{4}$$
$$=\operatorname{tr}T^N \tag{5}$$

By diagonalizing $\boldsymbol{T}$, Z is written as $\sum_{i=1}^{4}\lambda_i^N$ where λ_i are the eigenvalues of $\boldsymbol{T}$. Therefore, the free energy per spin pair, $(1/N)$, is approximated by the largest eigenvalue among λ_i's in the thermodynamic limit $N\rightarrow\infty$. In calculating the eigenvalue, we assume $-j_1>>-j_2>0$, and expand it in terms of the parameter $\varepsilon\equiv e^{\frac{1}{2}J_1}$ the expansion being effective at low temperatures. An analytic expression for the magnetic susceptibility χ per spin pair is obtained at the first lowest non-trivial order of ε as follows,

$$\chi=k_BT\frac{\partial^2}{\partial\boldsymbol{H}^2}\frac{1}{N}\log\ Z|_{H=0} \tag{6}$$

$$\rightarrow\frac{g^2\mu_B^2}{k_BT}\{1\cdot e^{\frac{J_1}{2k_BT}}+(-4+3e^{\frac{J_2}{2k_BT}})(e^{\frac{J_1}{2k_BT}})^2+\cdots\}\quad(N\rightarrow\infty) \tag{7}$$

Acknowledgements

This work was partly supported by Ministry of Education, Science, Sports and Culture, Japan.

References

1 R. Allman, *Z. Krist.*, 1970, **132**, 129.
2 A. Camerman and J. Trotter, *Proc. R. Soc. London Ser. A*, 1964, **279**, 129; J. Tanaka, *Bull. Chem. Soc. Jpn.*, 1963, **36**, 1237; H. A. Kerr, *Acta. Crystallogr., Sect. A: Cryst. Phys. Diffr. Theor. Gen. Cryst.*, 1966, **21**, 119.
3 H. Kobayashi, A. Kobayashi, Y. Sasaki, G. Saito and H. Inokuchi, *Bull. Chem. Soc. Jpn.*, 1986, **59**, 301.
4 Y. Deng, A. J. Illies, M. A. James, M. L. McKee and M. Peschke, *J. Am. Chem. Soc.*, 1995, **117**, 420.

---

†CCDC reference number 1145/240. See http://www.rsc.org/suppdata/jm/b0/b004557h/ for crystallographic files in .cif format.

5 For a review see: M. R. Bryce, *J. Mater. Chem.*, 1995, **5**, 1481; K. Heuze, M. Fourmigue and P. Batail, *J. Mater. Chem.*, 1999, **9**, 2373.

6 J. A. K. Howard, A. S. Batsanov, M. R. Bryce, J. N. Heaton, A. E. Underhill and N. Robertson, *Acta Crystallogr., Sect. C: Cryst. Struct. Commun.*, 1994, **50**, 1956; J. A. K. Howard, A. S. Batsanov, M. R. Bryce, J. N. Heaton, A. E. Underhill and N. Robertson, *J. Mater. Chem.*, 1998, **8**, 1541.

7 A. Dolbecq, M. Fourmigué, P. Batail and C. Coulon, *Chem. Mater.*, 1994, **6**, 1413.

8 G. Ono, A. Izuoka, T. Sugawara and Y. Sugawara, *J. Mater. Chem.*, 1998, **8**, 1703.

9 L. Leiserowitz and G. M. J. Schmidt, *J. Chem. Soc. (A)*, 1969, 2372.

10 R. C. Wheland and J. L. Gillson, *J. Am. Chem. Soc.*, 1976, **98**, 3916.

11 J. B. Torrance, *Acc. Chem. Res.*, 1979, **12**, 79; J. B. Torrance, *Mol. Cryst. Liq. Cryst.*, 1985, **126**, 55.

12 M. Troyer, H. Tsunetsugu and D. Wurtz, *Phys. Rev. Sect. B*, 1994, **50**, 13515; T. M. Rice, S. Gopalan and M. Sigrist, *Europhys. Lett*, 1993, **23**, 445; T. Komatsu, N. Kojima and G. Saito, *Solid State Commun.*, 1997, **103**, 519; H. Imai, T. Otsuka, T. Naito, K. Awaga and T. Inabe, *J. Am. Chem. Soc.*, 1999, **121**, 8098; G. Rovira, J. Veciana, E. Ribera, J. Tarres, E. Canadel, R. Rousseau, M. Mas, E. Molins, M. Almedia, R. T. Henriques, J. Morgado, J.-P. Schoeffel and J.-P. Pouget, *Angew. Chem., Int. Ed. Engl.*, 1997, **36**, 2324.

13 M. C. Burla, M. Camalli, G. Casacrano, C. Giacovazzo, G. Polidori, R. Spagna and D. Viterbo, *J. Appl. Crystallogr.*, 1989, **22**, 389.